0090-9556/91/1904-0740$03.00/0
DRUG METABOLISM AND DISPOSITION
Vol. 19, No. 4
Printed in U.S.A.

BIOTRANSFORMATION OF PRAVASTATIN SODIUM IN HUMANS

DONALD W. EVERETT, THEODORE J. CHANDO, GERALD C. DIDONATO, SAMPAT M. SINGHVI, HENRY Y. PAN, AND STEPHEN H. WEINSTEIN

Departments of Metabolism and Pharmacokinetics (D.W.E., T.J.C., S.M.S., S.H.W.), Analytical Research (G.C.D.), and Human Pharmacology (H.Y.P.), The Bristol-Myers Squibb Pharmaceutical Research Institute

(Received February 6, 1991; accepted February 26, 1991)

ABSTRACT:

Pravastatin sodium (PV) is a potent cholesterol-lowering agent that acts by inhibiting 3-hydroxy-3-methylglutaryl-coenzyme A reductase. Biotransformation profiles of PV in pooled human urine, plasma, and feces from healthy male volunteers given single 19.2-mg oral or 9.9-mg iv doses of [^{14}C]PV were determined by HPLC. The predominant drug-related component in urine, plasma, and feces corresponded to intact PV; in the pooled urine samples, PV constituted 29 and 69% of the radioactivity after the po and iv doses, respectively. The $\Delta^{4,5}$-3α-hydroxy isomer of PV constituted 10% (po) and 2% (iv), and 6-epi-PV constituted 3% (po) and 1% (iv) of the urinary radioactivity. Negligible amounts of the lactones of PV or its isomers were detected in urine, plasma, or feces. At least 15 other metabolites were also present; none of these accounted for more than 6% of the total urinary radioactivity. For metabolite isolation, an aliquot of pooled urine samples, obtained after administration of the radioactive dose, was added as a tracer to urine samples obtained from healthy subjects after administration of single nonradiolabeled 40-mg oral doses of PV. Urinary metabolites were concentrated on an XAD-2 column, extracted with ethyl acetate, and purified by extensive preparative HPLC. In addition to isolation and identification of unchanged drug and the two isomeric metabolites described above, eight other metabolites were isolated and structural assignments were made based on HPLC, UV spectra, mass spectral analysis, and proton NMR. Biotransformation pathways elucidated for PV include: (a) isomerization to 6-epi-PV and the 3α-hydroxy isomer of PV; (b) enzymatic ring hydroxylation; (c) ω-1 oxidation of the ester side chain; (d) β-oxidation of the carboxy side chain; (e) ring oxidation followed by aromatization; (f) oxidation of a hydroxyl group to a keto group; and (g) conjugation.

PV[1] (SQ 31,000, CS-514), a competitive inhibitor of HMG-CoA reductase, the rate-limiting enzyme in cholesterol biosynthesis, has been demonstrated to effectively reduce plasma cholesterol in animal studies (1) and in clinical trials (2–4). PV is designated chemically as 1,2,6,7,8,8a-hexahydro-β,δ,6-trihydroxy-2-methyl-8-(2-methyl-1-oxobutoxy)-1-naphthaleneheptanoic acid, monosodium salt (fig. 1). The numbering of PV and related structures is that of Alberts *et al.* (5). Results of preclinical and early clinical studies of PV, including the metabolism of PV in rats, dogs, and monkeys and in isolated rat hepatocytes, have been published (6–9). Two isomers of PV, 3α-iso-PV and 6-epi-PV, as well as a triol metabolite, have been reported to be metabolites of PV in humans (7, 10). The absorption, bioavailability, elimination, and pharmacokinetics of PV in healthy subjects have been determined (3, 11). This report describes the isolation and identification of the metabolites of PV from human urine and the quantification of some of these metabolites in plasma, urine, and feces after oral and iv administration of [^{14}C]PV to humans.

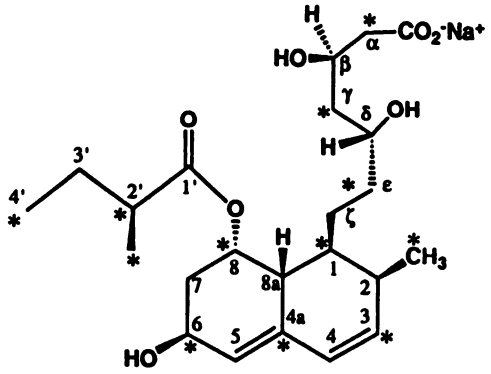

FIG. 1. *Structure of pravastatin sodium.*
The sites labeled with ^{14}C are indicated by *asterisks.*

Portions of this work were presented at the Third North American ISSX Meeting, "Modern Perspectives in Xenobiotic Metabolism," San Diego, CA, October 21–25, 1990.

[1] Abbreviations used are: PV, pravastatin, pravastatin sodium; PV-L, the δ-lactone of pravastatin; 3α-iso-PV, 3α-hydroxy-iso-$\Delta^{4,5}$-pravastatin; 3α-iso-PV-L, the δ-lactone of 3α-hydroxy-iso-$\Delta^{4,5}$-pravastatin; 6-epi-PV, 6-epi-pravastatin; 6-epi-PV-L, the δ-lactone of 6-epi-pravastatin; triol, Δ^{4}-3α,5β,6β-trihydroxy-pravastatin; 3′(*S*)-OH-PV, 3′(*S*)-hydroxy-pravastatin; desacyl-PV, desacyl-$\Delta^{4a,8,8}$-dehydro-pravastatin; HMG-CoA, 3-hydroxy-3-methylglutaryl-coenzyme A; FAB, fast atom bombardment; TBA, tetrabutylammonium hydrogen sulfate; TEA, triethylamine; COSY, correlated spectroscopy.

Send reprint requests to: Dr. Donald W. Everett, Department of Drug Metabolism and Pharmacokinetics, The Bristol-Myers Squibb Pharmaceutical Research Institute, P.O. Box 4000, Princeton, NJ 08543-4000.

Materials and Methods

Chemicals. [^{14}C]PV (fig. 1), with a specific activity of 4.9 μCi/mg, was provided by Sankyo Co., Ltd. (Tokyo, Japan). The radiochemical purity of the [^{14}C]PV was greater than 97% as determined by HPLC. All synthetic reference standards, including nonradiolabeled PV, PV-L, 3α-iso-PV, 3α-iso-PV-L, 6-epi-PV, 6-epi-PV-L, triol, 3′(*S*)-OH-PV, 3′(*R*)-OH-PV, desacyl-PV, and 3,4-β-epoxy-PV, were also obtained from Sankyo. HPLC-grade solvents were used throughout. Reagent-grade tetrabutylammonium hydrogen sulfate was from Aldrich Chemical Co. (Milwaukee, WI) and TEA was obtained through Mallinckrodt Inc., (Paris, KY). Combined β-glucuronidase/sulfatase from *Helix pomatia* (type H-1, G 0751), phenolpthalein glucuronic acid, sodium salt (P

0376), and D-saccharic acid-1,4-lactone (S 0375) were obtained from Sigma Chemical Co. (St. Louis, MO).

Dosing and Sample Collection. In an open, balanced, randomized, two-way crossover study, each of eight healthy male subjects (age, 21 to 39 years; weight, 64 to 84 kg) received a single 19.2-mg oral dose (100 μCi) and a single 9.9-mg iv dose (25 μCi) of [^{14}C]PV on two different occasions separated by a "washout" period of 7 days. Urine, plasma, and fecal samples were collected for up to 4 days after drug administration. The detailed experimental protocol has been described elsewhere (11). HPLC biotransformation profiles were determined for representative pooled plasma, urine, and fecal samples from this radiolabeled study.

For isolation and identification of the metabolites of PV, a portion of the pooled urine samples (0 to 6 hr) from the clinical study that used radiolabeled PV (11) was added as a tracer to pooled urine samples (0 to 8 hr) obtained from a separate clinical study, in which 24 healthy male subjects were given single 40-mg oral doses of nonradiolabeled PV. The doses used in both clinical studies were within the therapeutic dosing range for PV.

Biotransformation Profiles. Samples of pooled plasma (1 hr), urine (0 to 48 hr), and fecal homogenates (0 to 96 hr) were mixed with 25 μl of an acetonitrile/water, 1:1 (v/v) solution containing about 25 μg each of the available synthetic reference standards (see "Chemicals" above) before HPLC analysis. After addition of the reference standards and after high speed centrifugation (10,000*g*), urine samples were injected directly into the HPLC. Plasma samples (2.0 ml) were deproteinized by adding 4.0 ml of acetonitrile followed by centrifugation for 10 min at 700*g*. After removal of the clear supernatant, the protein precipitate was washed twice with 2.0 ml of acetonitrile/water, 2:1 (v/v). The combined supernatants were evaporated to dryness *in vacuo* and reconstituted into 1.0 ml of acetonitrile/water, 2:1 (v/v). After high speed centrifugation, the supernatant was quantitatively removed, mixed with 0.5 ml of water, and recentrifuged at high speed. A 1.0-ml aliquot was injected into the HPLC.

Fecal homogenates (1.0 g) were mixed with 2.0 ml of acetonitrile and sonicated for 5 min. The sonicated mixture was then shaken in a wrist-action shaker for 20 min and then centrifuged for 10 min at 700*g*. The supernatant was decanted and saved. The precipitate was washed twice more with 1.0 ml of acetonitrile/water, 2:1 (v/v) and an aliquot (0.5 ml) of the combined supernatants was injected into the HPLC.

All HPLC analyses, as well as the preparative isolation of metabolites, were performed on a Hewlett-Packard model 1090A liquid chromatograph, equipped with a diode-array UV detector. Two different HPLC systems (A and B) were used to characterize the biotransformation profile of PV in pooled plasma, urine, and fecal samples. Both systems used a Whatman Partisil 10 ODS-3 Magnum 9 semipreparative reverse phase (C_{18}) column (9.4 mm × 50 cm, Whatman Inc., Clifton, NJ) equipped with a guard column. For HPLC system A, the mobile phase consisted initially of 25% acetonitrile/75% 0.01 M potassium phosphate buffer (pH 7.2) containing 0.005 M TBA. This initial mobile phase was maintained for 25 min; the mobile phase was then changed in a linear gradient over a period of 45 min to a final composition of 50% acetonitrile/50% 0.01 M potassium phosphate buffer (pH 7.2) containing 0.005 M TBA. The final composition was maintained for an additional 10 min (total run time of 80 min).

HPLC system B consisted initially of 15% acetonitrile/85% 0.01 M potassium phosphate buffer (pH 7.2) containing 0.005 M TBA. The initial mobile phase was maintained for 20 min; the acetonitrile content of the mobile phase was then increased in a linear gradient over a period of 40 min to a final composition of 26% acetonitrile. In the final gradient step, the composition of the mobile phase was changed in a linear manner over a period of 15 min to give a final composition of 50% acetonitrile/50% 0.01 M potassium phosphate buffer (pH 7.2) containing 0.005 M TBA. The final composition of the mobile phase was maintained for 5 min to give a total run time of 80 min.

For both HPLC systems A and B, the mobile phase flow rate was 4 ml/min. Fractions of column effluent were collected for either 0.5- or 1-min intervals and each fraction was mixed directly with 15 ml of scintillation cocktail (Hydrocount; J. T. Baker, Phillipsburg, NJ) for determination of radioactivity by liquid scintillation counting.

Combined β-Glucuronidase/Sulfatase Enzyme Hydrolysis. Enzyme hydrolysis was performed using combined β-glucuronidase/sulfatase at a final concentration of 909 β-glucuronidase units/ml in 0.09 M sodium acetate, pH 4.8. Incubations were performed using phenolphthalein glucuronic acid as a positive control, and with the β-glucuronidase inhibitor, D-saccharic acid-1,4-lactone, added to selected incubations to differentiate sulfatase activity from β-glucuronidase activity.

Isolation of Metabolites from Human Urine. The overall scheme used for the isolation of the metabolites of PV from human urine is shown in fig. 2. Briefly, a total volume of 14 liters of urine was applied, 2 liters at a time, to a column of XAD-2 resin (4.3 × 40 cm). After washing the column with 1 liter of water, the radioactive metabolites were eluted with 1 liter of acetonitrile, followed by 1 liter of 80% acetonitrile in water. The recovery of radioactivity from the XAD column averaged 95%. The acetonitrile and acetonitrile/water eluents were combined and concentrated *in vacuo*. After addition of 36 ml of 0.2 M potassium phosphate buffer (pH 3.0) and 178 g of sodium chloride to the concentrated aqueous extract (177 ml), the solution was adjusted to pH 3.0 by dropwise addition of 0.5 N hydrochloric acid, while rapidly stirring the solution. This buffered solution was extracted 3 times with 2 volumes of ethyl acetate (total recovery 77%). Each ethyl acetate extract was immediately neutralized by addition of 2.0 ml of TEA. HPLC analysis of the aqueous and combined ethyl acetate fractions in both systems A and B indicated that all but the most polar metabolites were well extracted. The combined ethyl acetate extracts were concentrated *in vacuo* to 4.5 ml of a brown, oily liquid, which contained mostly water. Water (6.3 ml) was added to the concentrate, followed by 2.0 ml of acetonitrile/water, 15:85(v/v). This concentrated extract was separated into its radioactive constituents by multiple injections of aliquots (0.9 ml) into HPLC system B (Whatman column); 1-min fractions were collected for each run. A small aliquot of each fraction (25 μl) was combined with Hydrocount (J. T. Baker) and the radioactivity in each fraction was determined by use of a liquid scintillation counter. Individual fractions from each run were combined according to retention time into two major fractions, designated fraction 1 and fraction 2, which constituted 22 and 68%, respectively, of the radioactivity recovered from the column. Fraction 1 con-

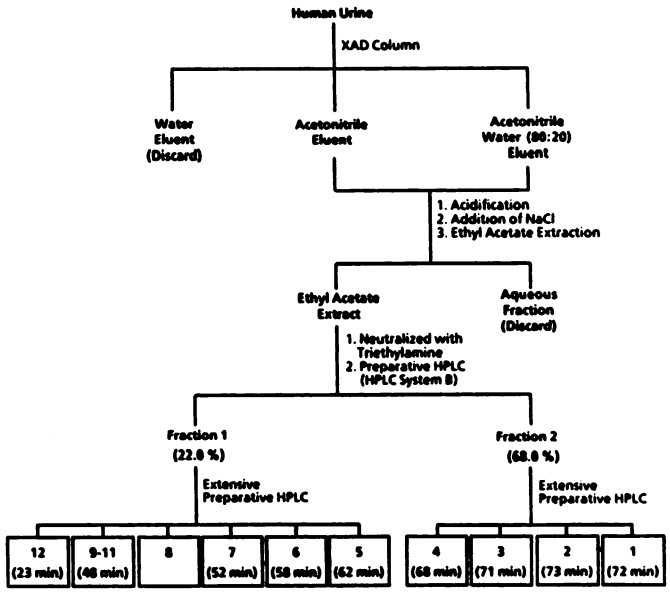

FIG. 2. *Scheme for the isolation and purification of pravastatin metabolites from human urine.*

The approximate retention times of the metabolites in HPLC system B are shown in parentheses. Since metabolite 8 was consumed in identification attempts, its retention time in HPLC system B was not determined.

tained many minor polar metabolites, while fraction 2 contained PV and less-polar metabolites. These two major fractions were further purified by repeated preparative HPLC until the diode-array detector indicated a high degree of purity for each metabolite. Preparative HPLC was performed using either a semipreparative Whatman Partisil 10 ODS-3 M9 column (0.9 × 50 cm) or an analytical Beckman Ultrasphere ODS column (0.46 × 25 cm, 5 μm particle size). HPLC solvent systems consisted of mixtures of acetonitrile or methanol with a buffered aqueous phase containing either TEA (water/acetic acid/TEA, 670:1:1) or TBA (0.005 M TBA, 0.01 M potassium phosphate, pH 6.0) as ion pair reagents. Because the TEA mobile phase was somewhat acidic (pH 4.3), the fractions were immediately neutralized with a small aliquot of TEA (about 5 μl). After each preparative run, the mobile phase from combined fractions was evaporated *in vacuo*. After dissolving the residue in a small volume of water, removal of mobile phase buffer salts was accomplished by solid phase extraction on C_{18} Bond Elut cartridges manufactured by Analytichem International (Harbor City, CA). Prior to mass spectral or NMR analysis, isolated metabolites were converted to Na^+ salts by passage through a cation exchange column (0.4 × 4.0 cm) packed with Bio-Rad AG 50W-X2 resin.

Spectroscopy. UV spectra were obtained with the diode-array detector in the mobile phase composition in which they eluted from the HPLC.

Proton NMR spectroscopy was performed on either a Jeol GX-400 or a Jeol GSX-500. All compounds were dissolved in D_2O (99.96 atom % D; MSD Isotopes, Montreal, Canada). All chemical shifts (δ_H) are reported in ppm relative to tetramethylsilane as an internal reference. The standard COSY pulse sequence was used for two-dimensional spin correlation experiments. Interpretable COSY spectra were obtained on as little as 65 μg.

Mass spectrometry was performed on either a VG-ZAB-2F or a Sciex API-III Triple Quadrupole mass spectrometer. FAB mass spectrometry was performed on the VG-ZAB-2F. Conditions were as follows: accelerating voltage was 8 kV; FAB matrices consisted of dithiothreitol, dithioerythritol, dimethylsulfoxide, and glycerol; the MS/MS collision gas was air, and the collision energy was 8 keV. The Sciex API-3 triple quadrupole employed ion spray as the ionization technique; this technique produces gas phase ions from charged species in solution (12). A 50 ng/ml solution of metabolite in methanol was introduced into the mass spectrometer at a flow rate of 3 μl/min. The MS/MS collision gas was argon and the collision energy was 50 eV.

Results

Biotransformation profiles of pooled urine (0–48 hr) from eight healthy male volunteers given a 19.2-mg dose of [^{14}C]PV are shown in fig. 3. Reference standards or previously isolated metabolites were co-injected with the pooled human urine obtained after administration of [^{14}C]PV for determination of the relative amount of each metabolite in the human urine sample. The retention times of these metabolites are indicated in fig. 3 and the relative distribution of each metabolite in pooled urine (0–48 hr), plasma (1 hr), and feces (0–96 hr) is summarized in table 1. HPLC system A (fig. 3, upper chromatogram) gave good resolution among PV, 3α-iso-PV, 6-epi-PV, and the lactone of PV; the lactones of 3α-iso-PV and 6-epi-PV were separated from the other compounds, but not from each other. The major radioactive component in the pooled urine, constituting 29 and 69% of the radioactivity after the po and iv doses, respectively, corresponded to intact PV (table 1). The corresponding values for 3α-iso-PV were 10% (po) and 2% (iv) and for 6-epi-PV were 3% (po) and 1% (iv). Negligible amounts of the lactones of PV or its isomers were detected in urine, plasma, or feces. The polar biotransformation products were not well separated in this HPLC system. For more detailed characterization of the polar biotransformation products, HPLC system B was used (fig. 3, lower chromatogram). At least 15 metabolites more polar than PV

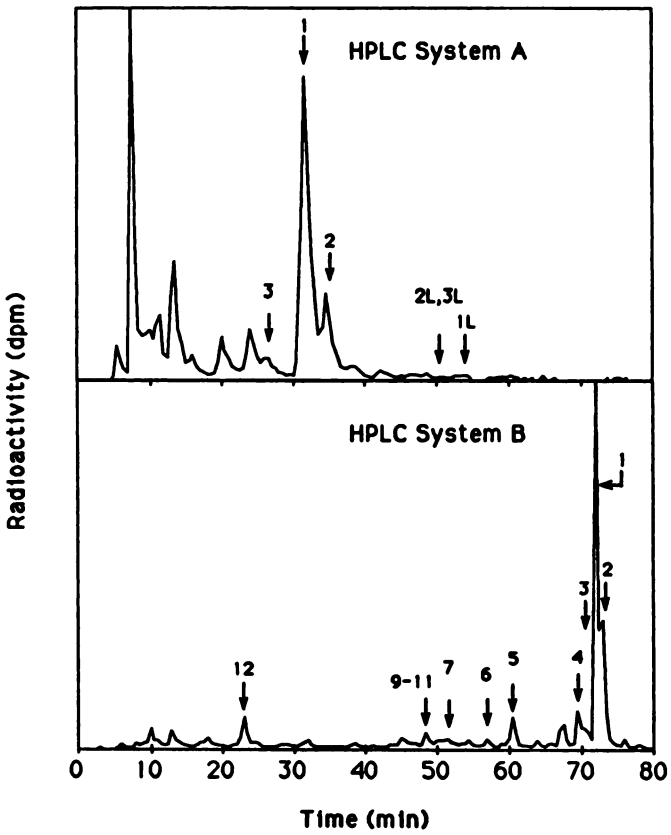

FIG. 3. *Biotransformation profiles of pooled human urine samples as determined by HPLC systems A (upper) and B (lower).*

The retention times of isolated metabolites and reference standards that were co-injected with the human urine samples are indicated by *arrows*; the *arabic numerals* refer to the structures in fig. 5. The lactones of PV, 3α-iso-PV, and 6-epi-PV are designated *1L*, *2L*, and *3L*, respectively.

were present in the pooled human urine; none of these accounted for more than about 6% of the urinary radioactivity.

For metabolite isolation, an aliquot of the urine collected from subjects given the radioactive dose of PV was added as a tracer to urine samples obtained from healthy subjects after administration of single nonradiolabeled 40-mg doses of PV. Urinary metabolites were concentrated on an XAD-2 column. The concentrated extract was acidified to pH 3.0, extracted with ethyl acetate, and the ethyl acetate extract was purified further by extensive preparative HPLC to give metabolites **1** to **12** (fig. 2). Because of the tendency of PV and related compounds to isomerize in acid (7), precautions were taken to minimize the exposure to acidic conditions throughout the isolation of the metabolites from human urine. For example, because the TEA mobile phase was mildly acidic (pH 4.3), the fractions obtained after a preparative run with this system were immediately neutralized with a small aliquot of TEA. In addition, the effect of acidification of the XAD extract to pH 3.0 prior to ethyl acetate extraction was tested on a small aliquot before the entire extract was committed to this procedure. The HPLC profiles before and after the extraction were the same. In spite of these precautions, metabolite **3** was unstable during isolation attempts.

NMR spectral data are summarized in table 2. The NMR spectral data for PV and 3α-iso-PV were in good agreement with the published NMR spectral data (13). Proton NMR spectra of the metabolites were assigned by comparison with the spectra of

TABLE 1

Biotransformation profiles of pravastatin in representative pooled plasma, urine, and fecal samples, as determined by HPLC, after a single 9.9-mg iv and 19.2-mg oral dose of [^{14}C]pravastatin to healthy subjects

Metabolites 1, 2, and 3 and their respective lactones (not shown) were determined in HPLC system A; the three lactones collectively accounted for less than 1% of the radioactivity in any sample. Metabolites 4 through 12 were determined in HPLC system B.

Metabolite	Reference Compound	Percentage Distribution of Radioactivity					
		Plasma (1 hr)		Urine (0–48 hr)[a]		Feces (0–96 hr)[a]	
		iv	po	iv	po	iv	po
1	PV	42.1	23.7	68.6	29.0	66.2	47.6
2	3α-iso-PV	4.5	23.7	2.3	10.0	8.2	13.9
3	6-epi-PV	0.0	1.0	1.3	2.8	0.0	0.7
4	Desacyl-PV	6.1	6.8	2.5	5.0	[b]	[b]
5		[c]	[c]	1.4	4.9	[b]	[b]
6		[c]	[c]	0.5	0.8	[b]	[b]
7	3′(*S*)-OH-PV	1.5	0.6	2.2	3.3	[b]	[b]
8		[c]	[c]	[d]	[d]	[b]	[b]
9–11[e]		[c]	[c]	2.7	6.2	[b]	[b]
12	Triol	8.0	3.3	3.3	6.2	[b]	[b]

[a] Recoveries of the radioactive doses were 20% (po) and 59% (iv) in urine; 71% (po) and 34% (iv) in feces.

[b] Feces were analyzed only in HPLC system A.

[c] The isolated metabolites were not co-chromatographed in plasma.

[d] The small amount of metabolite 8 isolated was consumed in identification attempts; therefore, it was not co-chromatographed with urine.

[e] Metabolites 9, 10, and 11 were not completely resolved in HPLC system B, so the value shown is the total of all three metabolites.

PV and the other reference standards available. The olefinic protons of the *trans*-diene and any oxygen-bearing methine protons were clearly observed downfield in the NMR spectra of these metabolites. In addition, the two methyl groups of the oxybutoxy side chain (2′-Me, 3′-Me) and the methyl group (2-Me) of the decalin ring structure were observed at the high-field end of the spectra in all cases. The UV spectra were very useful for the assignment of a unique structure to each metabolite. Among the 12 isolated compounds, 4 distinct UV spectra were observed by use of the diode-array detector (fig. 4).

Structures of the metabolites of PV are shown in fig. 5. Of the 11 compounds identified, reference standards of known stereochemistry were available for 6 of them. Proton NMR, mass spectral fragmentation patterns, UV spectra, and HPLC characteristics could be compared with these six reference compounds. Structural assignment of metabolites for which no reference standard was available was based on interpretation of the NMR (including COSY), mass, and UV spectra. FAB mass spectra were successfully obtained for four of the isolated metabolites, but the technique was found to lack the sensitivity required for obtaining interpretable spectra for most of the minor metabolites. For this purpose, the ion spray technique (nebulizer-assisted electrospray) was found to give excellent sensitivity (daughter ion spectra could be obtained on as little as 10 ng of reference compound) with a significant improvement in signal-to-noise over that obtained with FAB spectra. Generally, the MS/MS spectrum of the $(M - H)^-$ ion was used for identification purposes. The significant daughter ions for PV and some of its metabolites are shown in table 3. The daughter ion resulting from the loss of the 2-methylbutyryl side chain (m/z 101 for PV), and the alternate ion, with charge retention on the remaining portion of the molecule (m/z 321 for PV), allowed the determination of any modification to the ester side chain. The daughter ion resulting from loss of the ester side chain and the cleavage of the heptanoate side chain between the γ and δ carbon atoms, followed by a further loss of water (m/z 199 for PV), allowed the determination of any modifications to the decalin ring system. The evidence and rationale for the assignment of the 12 metabolites follows.

Metabolite 1. This compound had the same retention time as unchanged PV in HPLC systems A and B (fig. 3). The UV spectrum (fig. 4*A*) and the proton NMR (table 2) were identical to that of PV. The FAB mass spectra showed ions at m/z 447 $(M + Na)^+$, and 469 $(M + 2Na)^+$ in the positive mode and at m/z 423 $(M - H)^-$ in the negative mode. The daughter ion spectrum (MS/MS) of the parent ion of m/z 447 was similar to that of authentic PV. These results confirmed the identity of metabolite 1 as unchanged PV.

Metabolite 2. This metabolite had the same retention time as 3α-iso-PV in HPLC systems A and B (fig. 3). The UV spectrum (fig. 4*A*) and the proton NMR (table 2) were identical to that of 3α-iso-PV. The FAB mass spectra showed an ion at m/z 447 $(M + Na)^+$, and 469 $(M + 2Na)^+$in the positive mode and at m/z 423 $(M - H)^-$ in the negative mode. The daughter ion spectrum (MS/MS) of the parent ion of m/z 447 was similar to that of authentic 3α-iso-PV. These results confirmed the identity of metabolite 2 as 3α-iso-PV.

Metabolite 3. This metabolite had the same retention time as 6-epi-PV in HPLC systems A and B (fig. 3); the UV spectrum was also the same (fig. 4*A*). This compound decomposed during successive preparative HPLC attempts until insufficient sample remained for direct identification. When the reference standard 6-epi-PV was treated in a similar manner (*i.e.* simulated isolation) to that of metabolite 3, a similar decomposition was observed. As described previously, the mildly acidic mobile phase (pH 4.3) was neutralized with TEA prior to evaporation of the mobile phase during the isolation procedure; when the mobile phase was not neutralized with TEA prior to evaporation during a simulated isolation using authentic 6-epi-PV, the decomposition was increased. Since 6-epi-PV is known to undergo an allylic rearrangement similar to PV under acidic conditions (7), we suspected that the primary decomposition product was 3α-iso-PV. This was confirmed by co-chromatography of the decomposition product with 3α-iso-PV in a reverse phase HPLC system; the UV spectrum was also the same as that of 3α-iso-PV. Since 6-epi-PV has been identified previously as a metabolite of PV in humans, these results confirmed the identity of metabolite 3 as 6-epi-PV.

Metabolite 4. This metabolite had the same retention time as desacyl-PV in HPLC system B (fig. 3). The UV spectrum of metabolite 4 was also similar to that of desacyl-PV (fig. 4*C*) and quite different from PV or any of the other isolated metabolites. The FAB mass spectrum showed ions at m/z 321 and 319 in the positive and negative modes, respectively, which were attributed to the $(M + H)^+$ and $(M - H)^-$ ions of a compound of molecular weight 320. Metabolite 4 co-chromatographed with authentic desacyl-PV on reverse phase HPLC, and the NMR spectrum of the metabolite and the standard were identical. Based on these data, metabolite 4 was identified as desacyl-PV.

Metabolite 5. The UV spectrum of metabolite 5 was similar to that of PV (fig. 4*A*). The proton NMR spectrum was similar to that of PV, but with signals for five additional protons present between δ 3.2 and 4.6 ppm (table 2). The five oxygen-bearing

TABLE 2

Proton NMR of pravastatin and its metabolites determined in deuterium oxide

Values are chemical shifts (ppm).

^1H	PV (1)	3α-iso-PV (2)	Desacyl-PV (4)	PV-Glucuronide (5)	5,6-epoxy-3α-iso-PV (6)	3′(*S*)-OH-PV (7)	Tetranor Conjugate (8)	3′(*S*)-OH-PV Tetranor (9)	3-keto-5,6-diol (10)	7-OH-3α-iso-PV (11)	Triol (12)
1	1.61	1.73	2.59	1.59	1.93	~1.58[a]	[b]	[b]	[b]	1.77	1.69
2	2.41	1.95	2.59	2.42	2.03	~2.45	~2.49	~2.47	[b]	1.98	1.88
3	6.01	3.96	5.92	6.02	3.98	6.01	6.01	6.01		4.00	3.89
4	6.04	5.66	6.35	6.04	6.27	6.04	6.04	6.04	6.07	5.81	5.89
5	5.54	6.16	6.61	5.65	3.73	5.53	5.53	5.53	4.42	6.33	4.21
6	4.36	5.72		4.47	3.55	4.39	4.36	4.38	3.84	5.78	3.89
7	2.44	2.49	7.08	2.50	2.28	~2.45	~2.49	~2.47	[b]	4.12	1.94
	1.64	2.36		1.73	2.28	~1.58	[b]	[b]	[b]		1.94
8	5.37	5.41	6.67	5.38	5.19	5.38	5.35	5.36	5.43	5.19	5.32
8a	2.47	2.25		2.48	2.15	~2.45	~2.49	~2.47	[b]	2.39	2.24
2-Me	0.85	0.72	0.93	0.83	0.73	0.84	0.85	0.85	0.99	0.75	0.73
α	2.31	2.33	2.29	2.30	2.36	2.31			2.33	2.33	2.32
	2.28	2.29	2.25	2.26	2.32	2.29			2.29	2.30	2.29
β	4.04	4.06	4.01	4.03	4.09	4.04			3.99	4.06	4.06
γ	1.58	1.61	~1.56	~1.57	1.63	~1.58			1.58	1.61	1.59
	1.58	1.61	~1.56	~1.57	1.63	~1.58			1.58	1.61	1.59
δ	3.66	3.73	3.63	3.66	3.76	3.68			3.70	3.75	3.72
ε	~1.52	~1.51	~1.56	~1.50	~1.57	~1.50	[b]	[b]	~1.48	~1.52	~1.53
	~1.52	~1.51	~1.56	~1.50	~1.57	~1.50	[b]	[b]	~1.48	~1.52	~1.53
ζ	~1.28	~1.31	1.39	~1.23	~1.30	~1.27	[b]	[b]	~1.25	~1.29	~1.35
	~1.28	~1.31	1.39	~1.23	~1.30	~1.27	[b]	[b]	~1.25	~1.29	~1.35
2′	2.39	2.38		2.40	2.41	~2.45	~2.49	~2.47	2.38	2.37	2.41
3′	1.53	1.51		~1.50	~1.57	3.85	3.96	3.84	~1.48	~1.52	~1.53
	1.43	1.43		1.41	1.48				1.43	1.43	1.45
2′-Me	1.06	1.02		1.03	1.08	1.11	1.12	1.11	1.04	1.02	1.06
3′-Me	0.81	0.78		0.79	0.83	1.04	1.08	1.04	0.77	0.78	0.80
a				4.53[c]							
b				3.26[c]							
c				3.60[c]							
d				3.43[c]							
e				3.43[c]							

[a] Due to the complexity of proton signals in the region δ 1.0–2.5, some chemical shift values are approximate. It is estimated that these values are accurate to within about 0.04 ppm.

[b] Assignment of these protons was not made because of multiple overlapping signals or interferring signals from minor impurities.

[c] The glucuronic acid protons.

methine protons of a glucuronide conjugate would be expected to give signals in this region of the spectrum. A COSY spectrum of the metabolite confirmed that these five protons were coupled in a manner consistent with glucuronic acid. The FAB mass spectrum showed ions at *m/z* 599 and 621 that were attributed to the $(M - H)^-$ and $(M + Na - 2H)^-$ ions of a compound of molecular weight of 600, which corresponds to the free acid form of PV-glucuronide. Exact mass determination of the $(M - H)^-$ ion resulted in a value of 599.2701 (599.2704 theoretical for PV-glucuronide). The ion spray mass spectrum showed ions at *m/z* 599 and 621 attributable to the $(M - H)^-$ and $(M + Na - 2H)^-$ ions, respectively, in agreement with the FAB mass spectrometry results. The daughter ion spectrum of the parent ion *m/z* 599 gave anion of *m/z* 193 indicative of the glucuronic acid moiety. When incubated with β-glucuronidase, the metabolite was hydrolyzed and the aglycone co-eluted with PV on reverse phase HPLC. This hydrolysis could be inhibited by addition of the β-glucuronidase inhibitor, D-saccharic acid-1,4-lactone, to the incubation mixture. Base hydrolysis under conditions (pH 12 for 2 hr at room temperature) known to hydrolyze acyl-linked β-glucuronide conjugates (14) did not hydrolyze metabolite **5**. A comparison of the chemical shifts of the protons in the NMR of metabolite **5** with those of PV showed a downfield shift of 0.12 ppm for the H_5 proton and 0.11 ppm for the H_6 proton of the metabolite relative to PV. This evidence, combined with the result of the base-hydrolysis experiment described above, suggested that the glucuronide group was conjugated at the 6-hydroxy position of PV and not at the carboxyl group or the β or δ hydroxy groups of the heptanoic acid side chain. Based on the above evidence, metabolite **5** was identified as PV-glucuronide.

Metabolite 6. The UV spectrum of this metabolite showed only end-absorption similar to that observed for the triol (fig. 4*B*). This indicated that the *trans*-diene system was no longer present in metabolite **6**. At most, a single olefin bond was present in the decalin ring structure. The ion spray mass spectrum showed ions at *m/z* 439 and 441 in the negative mode and the positive mode, respectively, which were attributed to the $(M - H)^-$ and $(M + H)^+$ ions corresponding to a metabolite with a molecular weight of 440. This difference of 16 mass units (PV, molecular weight = 424) suggests incorporation of oxygen into the molecule. The daughter ion spectrum resulting from the parent ion of *m/z* 439 gave a neutral loss of 102, indicative of an unmodified oxybutoxy side chain similar to PV. An ion of *m/z* 215 was indicative of one additional oxygen in the decalin ring structure; PV yielded an analogous ion at *m/z* 199. The

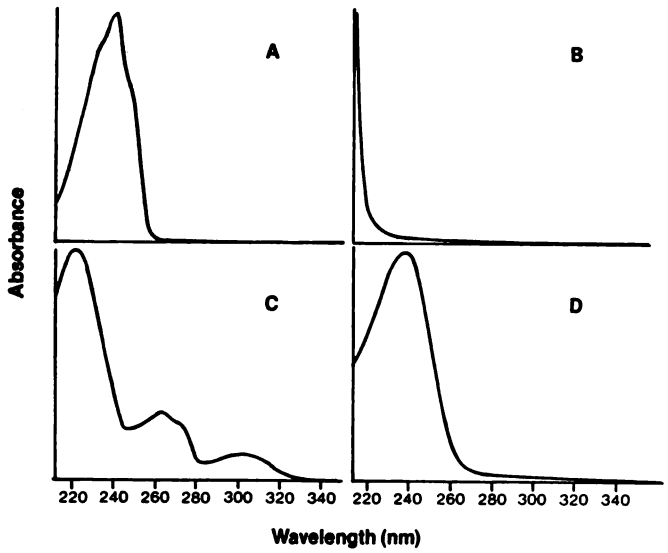

FIG. 4. *Absorbance spectra of pravastatin and some of its metabolites.*

The spectra were obtained in the mobile phase composition from which they eluted from the column. *A*, PV (1), 3α-iso-PV (2), 6-epi-PV (3), and 3′(*S*)-OH-PV (7); *B*,triol (12); *C*, desacyl-PV (4); *D*, metabolite 10.

proton NMR (table 2) showed only one olefinic proton present (δ 6.26, d). The midfield region of the NMR (δ 3.5–4.5) showed five oxygen-bearing methines. The chemical shifts and multiplicity of two of these protons were identical to the oxygen-bearing methines of the heptanoic acid side chain (H_β and H_δ) of PV, confirming that no modifications occurred on this side chain. A simple hydroxylation of the decalin ring system would result in only one additional oxygen-bearing methine proton. The loss of one double bond (from the UV spectrum) and the addition of a single oxygen atom to result in two additional oxygen-bearing methine protons suggest that an epoxide was formed. An authentic reference standard of 3,4-β-epoxy-PV (mol wt = 440) was available for comparison. Although the proton NMR was similar to that of metabolite **6**, there were substantial differences. The COSY spectrum showed a pronounced cross peak between the signal for the olefinic proton (δ 6.27) and one of the oxygen-bearing methine protons (δ 3.98) on the decalin ring and another pronounced cross-peak between the remaining two oxygen-bearing methine protons on the ring system (δ 3.73 and δ 3.55), indicating that these two pairs of protons were coupled. Based on these results, we concluded that metabolite **6** was 5,6-epoxy-3α-iso-PV. The stereochemistry of the epoxide group was not established.

Metabolite 7. This metabolite had the same retention time as 3′(*S*)-OH-PV in HPLC system B (fig. 3). The UV spectrum of metabolite 7 was also similar to that of 3′(*S*)-OH-PV (fig. 4*A*). The ion spray mass spectrum showed an intense ion at *m/z* 439 attributed to the $(M - H)^-$ ion of a compound of molecular weight 440, suggesting incorporation of an atom of oxygen into the molecule. The daughter ion spectrum of the ion of *m/z* 439 was similar to that of authentic 3′(*S*)-OH-PV. Significant daughter ions are indicated in table 3. Metabolite 7 co-chromatographed with authentic 3′(*S*)-OH-PV in a reverse phase system capable of separation of 3′(*S*)-OH-PV from its diastereomer with (*R*)-configuration at the 3′-position, which was also available as an authentic reference standard. The NMR spectra of metabolite

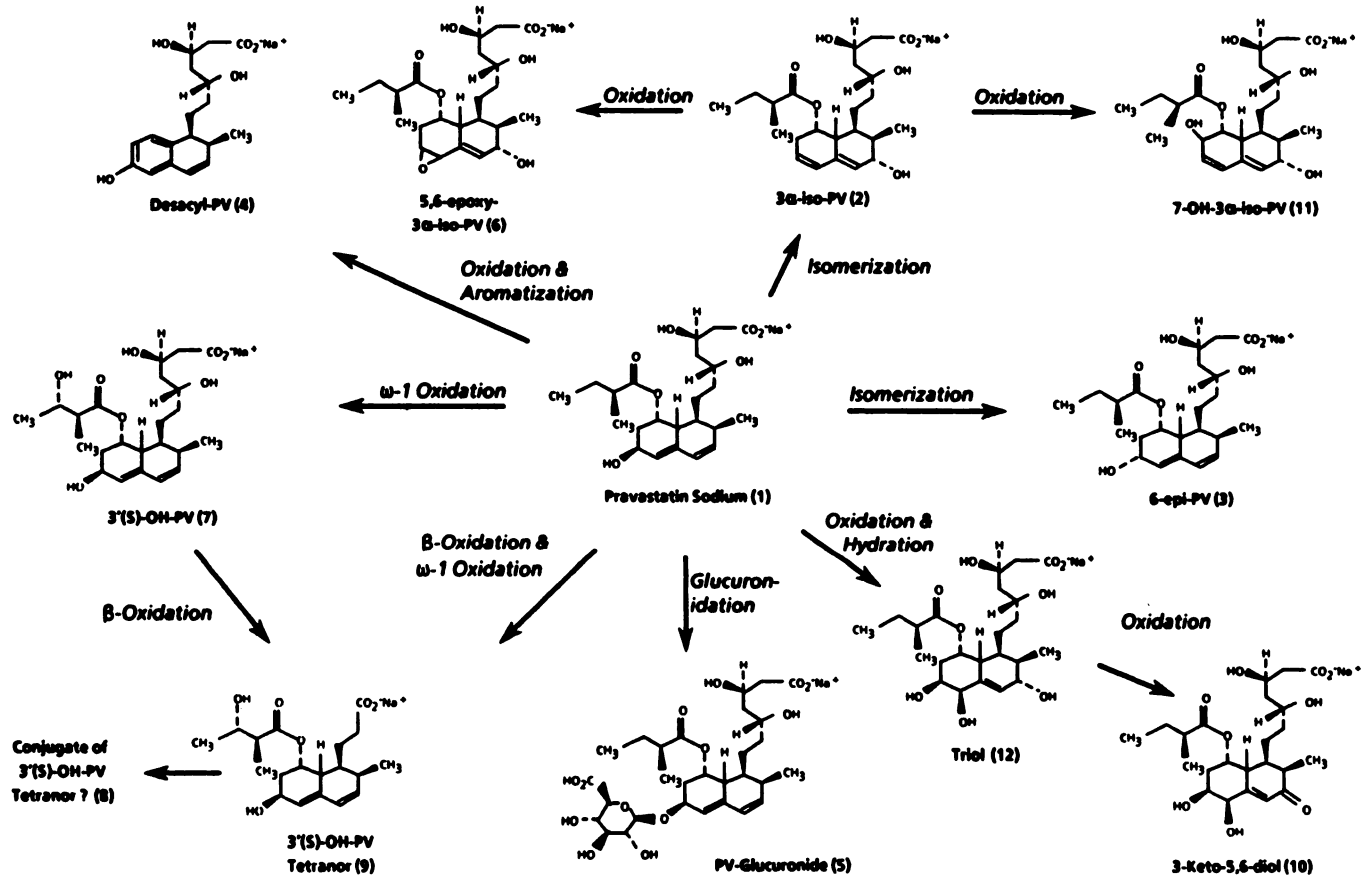

FIG. 5. *Biotransformation pathways for pravastatin in humans.*

TABLE 3

Significant daughter ions from the parent (M − H)⁻ ions generated by ion spray

Compound	Significant Daughter Ions[a]			
	Side Chain	Side Chain Loss	Decalin Ring Structure	(M − H)⁻
PV (**1**)[b]	101 (100)	321 (8)	199 (1)	423 (64)
3′(*S*)-OH-PV (**7**)[b]	117 (100)	321 (7)	199 (1)	439 (46)
Triol (**12**)[b]	101 (43)	355 (61)	233 (7)	457 (100)
7-OH-3α-iso-PV (**11**)	101 (81)	337 (14)	215 (100)	439 (50)
3-keto-5,6-diol (**10**)	101 (8)	353 (100)	231 (100)	455 (35)
3′(*S*)-OH-PV tetranor (**9**)	117 (100)	233 (1)		351 (2)
Tetranor conjugate (**8**)[c]	117 (100)	233 (6)		601 (13)
PV-glucuronide (**5**)[d]				599 (100)
5,6-epoxy-3α-iso-PV (**6**)	101 (5)	337 (6)	215 (10)	439 (100)

[a] The intensity of each ion as a percentage of the base peak is indicated in parentheses.

[b] These reference standards were run to identify the characteristic fragmentation pattern of these series of compounds.

[c] A 351 ion was a major ion in this spectrum (75% of the base peak) and was attributed to an ion with the structure of the tetranor of 3′(*S*)-OH-PV.

[d] An intense 193 ion (32% of the base peak) indicative of a glucuronide was observed.

7 and authentic 3′(*S*)-OH-PV were identical, confirming the identity of metabolite **7** as 3′(*S*)-OH-PV.

Metabolite 8. The UV spectrum of metabolite **8** was similar to that observed for PV (fig. 4*A*), indicating a conjugated *trans*-diene system present in the decalin ring. The ion spray mass spectrum yielded negatively charged ions at *m/z* 455, 479, 497, 499, and 601. None of these, except the ion at *m/z* 601, appeared to be related to PV when selected for MS/MS. The MS/MS spectrum of the ion of *m/z* 601 gave significant daughter ions *m/z* 351, 233, and 117 (table 3). This latter ion suggests oxidation of the 2-methylbutyryl side chain similar to that observed for 3′(*S*)-OH-PV. Except for the parent ion (*m/z* 601), the daughter ion spectrum was similar to that of metabolite **9**, which was identified as the tetranor analog of 3′(*S*)-OH-PV, suggesting that metabolite **8** was a conjugate of 3′(*S*)-OH-PV, with the loss of the conjugating moiety (neutral loss of 250 amu) resulting in the ion *m/z* at 351. Although impurities were evident in the proton NMR spectrum of metabolite **8** (table 2), the spectrum was similar to that of the tetranor of 3′(*S*)-OH-PV. Based on these data, metabolite **8** appears to be an unknown conjugate of metabolite **9** [tetranor of 3′(*S*)-OH-PV], although the identity of the conjugating group could not be determined.

Metabolite 9. The UV spectrum of metabolite **9** was similar to that observed for PV (fig. 4*A*), indicating a conjugated *trans*-diene system present in the decalin ring. The ion spray mass spectrum showed an intense ion at *m/z* 351, attributed to the (M − H)⁻ ion of a compound with a molecular weight of 352. The MS/MS spectrum of metabolite **9** yielded an ion at *m/z* 117 indicative of hydroxylation of the 2-methylbutyryl side chain. The daughter ion at *m/z* 233 resulted from the loss of this side chain (table 3). The proton NMR was similar to that of 3′(*S*)-OH-PV, with the exception that the signals for the oxygen-bearing methines of the heptanoic acid side chain (H_β and H_δ) were absent from the NMR spectrum. Based on these results, we concluded that metabolite **9** was the tetranor analog of 3′(*S*)-OH-PV.

Metabolite 10. The UV spectrum of metabolite **10** (fig. 4*D*) was somewhat similar to that observed for PV (fig. 4*A*), but without the fine structure characteristic of the *trans*-diene system. The ion spray mass spectrum showed an intense ion at *m/z* 455 attributed to the (M − H)⁻ ion of a compound with a molecular weight of 456. The observed loss of 102 (*m/z* 101 ion) from the parent to yield a daughter ion at *m/z* 351 in the MS/MS spectrum indicated that the 2-methylbutyryl side chain was unchanged (table 3). The intense daughter ion at *m/z* 231 was 2 amu less than required by the addition of two oxygen atoms to the decalin ring system of PV. The proton NMR showed two downfield protons at δ 6.07 and 5.43. If the proton at δ 5.43 is attributable to the H_8 proton, then only one olefinic proton is present in this compound. The three methyl groups were observed in the upfield region of the NMR and the H_β and H_δ oxygen-bearing methine protons were clearly visible. Relative to the triol metabolite (**10**), the 2-methyl group was shifted downfield by 0.26 ppm, indicating a substantial change in the neighborhood of the 2-methyl group. Based on these results, we concluded that metabolite **10** was the 3-keto-5,6-dihydroxy derivative of PV.

Metabolite 11. The UV spectrum of metabolite **11** was similar to that observed for PV (fig. 4*A*), indicating a conjugated *trans*-diene system present in the decalin ring. The ion spray mass spectrum showed an intense ion at *m/z* 439 attributed to the (M − H)⁻ ion of a compound with a molecular weight of 440, suggesting incorporation of an atom of oxygen into the molecule. The daughter ion spectrum of the ion of *m/z* 439 showed ions at *m/z* 101 and 215 (table 3), indicating that the oxygen atom was incorporated into the decalin ring system. The proton NMR spectrum was somewhat similar to that of 3α-iso-PV; the primary difference was an additional signal in the midrange of the spectrum (δ 4.12) attributed to an oxygen-bearing methine proton. The COSY spectrum showed intense cross-peaks between the proton at δ 4.12 and the signals attributed to the H_6 and H_8 protons, confirming that the hydroxyl group was at the 7-position. Based on these results, we concluded that metabolite **11** was 7-OH-3α-iso-PV. The stereochemistry at the 7-position was not determined, but due to steric considerations the hydroxyl would be expected to be β- to the decalin ring system.

Metabolite 12. This metabolite had the same retention time as the authentic triol reference standard in HPLC system B (fig. 3). The UV spectrum (fig. 4B) and the proton NMR (table 1) were identical to the triol. The FAB mass spectra showed ions at *m/z* 459 $(M + H)^+$ and 481 $(M + Na)^+$ in the positive mode and at *m/z* (M − H)⁻ in the negative mode, indicating a compound of molecular weight 458. This suggests the addition of two oxygen and two hydrogen atoms to PV. The daughter ion spectrum (MS/MS) of the ion of *m/z* 457 was the same as that of the authentic triol. The proton NMR spectra of metabolite **12** and the triol were also identical. These results confirmed the identity of metabolite **12** as the triol metabolite of PV.

Discussion

The major drug-related component found in plasma, urine, and fecal samples from healthy volunteers was intact PV. The major metabolite of PV in humans, confirmed by isolation from pooled urine samples, was 3α-iso-PV (**2**), which along with the triol (**12**) and 6-epi-PV (**3**) had been previously identified as a metabolite of PV in rats, dogs, monkeys, and humans (6, 7). Serum and urinary concentrations of 3α-iso-PV and the triol have been determined in clinical studies by a specific GC/MS method (3, 10, 15). Because of the tendency of PV to isomerize under acidic conditions (7), it is possible that both 3α-iso-PV

and 6-epi-PV are generated from PV by a nonenzymic acid-catalyzed reaction in the stomach before absorption from the gastrointestinal tract. Both lovastatin and simvastatin, HMG-CoA reductase inhibitors similar in structure to PV, are metabolized *in vivo* and *in vitro* to a 3α-hydroxylated product, analogous to 3α-iso-PV (16–18). The formation of this 3α-hydroxylated product from lovastatin and simvastatin was attributed to isomerization (*via* an allylic rearrangement) of the initially-formed 6β-hydroxylated metabolite under the acidic conditions employed for the isolation. During all procedures used in the present study, care was taken to minimize the exposure of PV and its metabolites to acidic conditions, because of the acid-catalyzed rearrangement possible with compounds of this general structure (7). While PV and 3α-iso-PV were stable during all procedures used for the isolation in the present study, metabolite **3** (6-epi-PV) was unstable and isomerized to the 3α-isomer during the attempted isolation. The instability of 6-epi-PV relative to PV and 3α-iso-PV can be explained by the stereochemistry and the mechanism of the isomerization. The most likely mechanism for the allylic rearrangement is as follows. First, the hydroxyl group at the 6-position is protonated. Then, in a concerted, or possibly in a step-wise fashion, a molecule of water is lost from the 6-position and a hydroxyl ion (or a water molecule) attacks the 3-position. The concerted mechanism would require only an incipient carbonium ion at the 6-position, while the step-wise mechanism would require generation of a full allylic carbonium ion. The 6α-hydroxy group in 6-epi-PV is in a 1,3-diaxial interaction with the very large 2-methylbutyryl group. The steric stress caused by this 1,3-diaxial interaction is relieved by the loss of a molecule of water from the 6-position and provides a driving force for the allylic rearrangement. The product of this rearrangement, 3α-iso-PV, has the hydroxy group on the opposite side of the ring from the adjacent methyl group and the large heptanoate side chain. The instability of the 6β-hydroxylated metabolites of lovastatin and simvastatin even under relatively mild conditions (16–18) can be similarly explained. In addition to the steric interaction between the 6α-methyl group the very large 2-methylbutyryl group, the methyl group present in lovastatin and simvastatin stabilize the incipient positive charge at the 6-carbon atom (3° carbonium ion) lowering the energy of the transition state. For these reasons, and because of the larger size of the methyl group relative to the hydroxyl group, the 6β-hydroxylated metabolites of lovastatin and simvastatin would be expected to be even more prone to isomerization than 6-epi-PV (2° carbonium ion).

A large number of other metabolites more polar than PV were present in urine and plasma. The desacyl metabolite (**4**) has been reported previously as a product that resulted from *in vitro* incubations of PV with isolated rat hepatocytes (9). Evidence was presented that this compound results from oxidation of the 6β-hydroxy to a ketone followed by spontaneous aromatization. Although no epoxides (*e.g.* **6**) have been previously identified as metabolites of PV either *in vivo* or *in vitro*, a 4a,5-β-epoxide of PV has been implicated as an intermediate in the formation of the triol and a glutathione conjugate (9).

Stereospecific ω-1 oxidation of PV was found to result in the formation of 3′(*S*)-OH-PV. Lovastatin also exhibited stereospecific formation of an analogous metabolite when incubated with rat or mouse liver microsomes, although the absolute chirality at the 3′-position was not determined (17, 19). The methyl group at the chiral center adjacent to the site of hydroxylation clearly directs the stereospecificity of this reaction, as indicated by the formation of both epimers of the 3′-hydroxylated metabolite when simvastatin is incubated with rat liver microsomes (18). Simvastatin possesses a 2,2-dimethylbutyryl side chain, while lovastatin and PV both possess a 2-methylbutyryl side chain with "S" stereochemistry at the 2-position; the additional methyl group at the 2′-position in simvastatin removes this chirality. Since the 2-methylbutyryl side chain of PV and lovastatin are of the same chirality, these results suggest that the 3′-hydroxylated metabolite of lovastatin possesses the "S" absolute configuration at the 3′-position similar to that observed for metabolite **7**.

The tetranor of 3′(*S*)-OH-PV (**9**) was presumably formed *via* two successive cycles of fatty acid β-oxidation of the heptanoic acid side chain. β-Oxidation appears to be ubiquitous for this class of compounds; a "pentanoic acid derivative" of lovastatin and simvastatin was isolated from livers of rodents treated with the hydroxy acid form of these HMG-CoA inhibitors. This metabolite was suggested to result from one cycle of β-oxidation followed by a reversal of the β-oxidation process, which resulted in the loss of the δ-hydroxy group (18). An analogous "pentanoic acid derivative" of PV has been isolated from rat plasma, and was present at lower concentrations in dog and monkey plasma, after administration of PV (7).

The triol and desacyl-PV were inactive when tested as inhibitors of HMG-CoA reductase, and 3α-iso-PV and 3′(*S*)-OH-PV had negligible activity (2 and 6%, respectively) relative to PV.[2] Only 6-epi-PV had any significant activity as an HMG-CoA reductase inhibitor (80% activity relative to PV), but it was only a minor metabolite of PV in humans. These results are consistent with those of a clinical study that showed that most of the inhibitory activity in serum after administration of PV was found to correspond to the parent drug (20). This is in contrast to lovastatin, where active metabolites other than lovastatin acid accounted for a substantial portion of the inhibitory activity after administration of lovastatin (20).

Acknowledgments. The authors would like to thank Dr. David A. Willard at the Clinical Pharmacology Unit of the Medical Center at Princeton and Dr. James T. Gourzis of Hill Top Pharmatest in Cincinnati, OH, for the clinical samples. The authors would also like to thank Mr. Mark Bolger (FAB/MS), Ms. Alicia Kahle (NMR), and Mr. Harold Malone (NMR), for their excellent technical assistance.

[2] C. P. Ciosek, unpublished results.

References

1. Y. Tsujita, M. Kuroda, Y. Shimada, K. Tanzawa, M. Arai, I. Kaneko, M. Tanaka, H. Masuda, C. Tarumi, Y. Watanabe, and S. Fujii: CS-514, a competitive inhibitor of 3-hydroxy-3-methylglutaryl coenzyme A reductase: tissue-selective inhibition of sterol synthesis and hypolipidemic effect on various animal species. *Biochim. Biophys. Acta* **877**, 50–60 (1986).
2. N. Nakaya, Y. Homma, H. Tamachi, H. Shigematsu, Y. Hata, and Y. Goto: The effect of CS-514 on serum lipids and apolipoproteins in hypercholesterolemic subjects. *J. Am. Med. Assoc.* **257**, 3088–3093 (1987).
3. H. Y. Pan, P. T. Funke, D. A. Willard, D. N. McKinstry: Pharmacokinetics, pharmacodynamics and safety of pravastatin sodium, a potent inhibitor of HMG-CoA reductase, in healthy volunteers. In "New Advances in the Control of Lipid Metabolism: Focus on Pravastatin" (J. C. LaRosa, ed.), pp. 9–21. Royal Society of Medicine Services Limited, London, 1989.
4. D. B. Hunninghake, M. J. Mellies, A. C. Goldberg, P. T. Kuo, J. B. Kostis, H. G. Schrott, W. Insull, H. Y. Pan: Efficacy and safety of

pravastatin in patients with primary hypercholesterolemia. II. Once-daily versus twice-daily dosing. *Arteriosclerosis* **85,** 257–262 (1990).

5. A. W. Alberts, J. Chen, G. Kuron, V. Hunt, J. Huff, C. Hoffman, J. Rothrock, M. Lopez, H. Joshua, E. Harris, A. Patchett, R. Monaghan, S. Currie, E. Stapley, G. Albers-Schonberg, O. Hensens, J. Hirshfield, K. Hoogsteen, J. Liesch, and J. Springer: Mevinolin: a highly potent competitive inhibitor of hydroxymethylglutaryl-coenzyme A reductase and a cholesterol-lowering agent. *Proc. Natl. Acad. Sci. U.S.A.* **77,** 3957–3961 (1980).
6. Y. Tsujita and Y. Watanabe: Pravastatin sodium: a novel cholesterol-lowering agent which inhibits HMG-CoA reductase. *Cardiovasc. Drug Rev.* **7,** 110–126 (1989).
7. M. Arai, N. Serizawa, A. Terahara, Y. Tsujita, M. Tanaka, H. Masuda, and S. Ishikawa: Pravastatin sodium (CS-514), a novel cholesterol-lowering agent which inhibits HMG-CoA reductase. *Sankyo Kenkyusho Nempo* **40,** 1–38 (1988).
8. T. Komai, K. Kawai, E. Shigehara, C. Kuroiwa, Y. Kawasaki, E. Kitazawa, and M. Tanaka: 2nd Int. ISSX Meeting entitled "Xenobiotic Metabolism and Disposition," Kobe, Japan, p. 121 (abstr.) (1988).
9. H. Takahagi, S. Muramatsu, K. Miyaguchi, I. Iwabuchi, T. Nakamura, T. Kinoshita, A. Kitagawa, Y. Matsushita, and M. Tanaka: 2nd Int. ISSX Meeting entitled "Xenobiotic Metabolism and Disposition," Kobe, Japan, p. 122 (abstr.) (1988).
10. P. T. Funke, E. Ivashkiv, M. E. Arnold, and A. I. Cohen: Determination of pravastatin sodium and its major metabolites in human serum/plasma by capillary gas chromatography/negative ion chemical ionization mass spectrometry. *Biomed. Environ. Mass Spectrom.* **18,** 904–909 (1989).
11. S. M. Singhvi, H. Y. Pan, R. A. Morrison, and D. A. Willard: Disposition of pravastatin sodium, a tissue-selective HMG-CoA reductase inhibitor, in healthy subjects. *Br. J. Clin. Pharmacol.* **29,** 239–243 (1990).
12. A. P. Bruins, T. R. Covey, and J. D. Henion: Ion spray interface for combined liquid chromatography/atmospheric pressure ionization mass spectrometry. *Anal. Chem.* **59,** 2642–2647 (1987).
13. H. Kuwano, N. Serizawa, K. Hamano, and A. Terahara: ^{1}H-NMR spectra of mono-hydroxy derivatives of ML-236B and MB-530B. *Sankyo Kenkyusho Nempo,* **37,** 147–154 (1985).
14. E. M. Faed: Properties of acyl glucuronides: implications for studies of the pharmacokinetics and metabolism of acidic drugs. *Drug Metab. Rev.* **15,** 1213–1249 (1984).
15. H. Y. Pan, A. R. DeVault, B. J. Swites, D. Whigan, E. Ivashkiv, D. A. Willard, and D. Brescia: Pharmacokinetics and pharmacodynamics of pravastatin alone and with cholestyramine in hypercholesterolemia. *Clin. Pharmacol. Ther.* **48,** 201–207 (1990).
16. M. D. Greenspan, J. B. Yudkovitz, A. W. Alberts, L. S. Argenbright, B. H. Arison, and J. L. Smith: Metabolism of lovastatin by rat and human liver microsomes *in vitro. Drug Metab. Dispos.* **16,** 678–682 (1988).
17. K. P. Vyas, P. H. Kari, S. M. Pitzenberger, R. A. Halpin, H. G. Ramjit, B. Arison, J. S. Murphy, W. F. Hoffman, M. S. Schwartz, E. H. Ulm, and D. E. Duggan: Biotransformation of lovastatin. I. Structure elucidation of *in vitro* and *in vivo* metabolites in the rat and the mouse. *Drug Metab. Dispos.* **18,** 203–211 (1990).
18. S. Vickers, C. A. Duncan, K. P. Vyas, P. H. Kari, B. Arison, S. R. Prakash, H. G. Ramjit, S. M. Pitzenberger, G. Stokker, and D. E. Duggan: *In vitro* and *in vivo* biotransformation of simvastatin, an inhibitor of HMG-CoA reductase. *Drug Metab. Dispos.* **18,** 476–483 (1990).
19. K. P. Vyas, P. H. Kari, S. R. Prakash, and D. E. Duggan: Biotransformation of lovastatin. II. *In vitro* metabolism by rat and mouse liver microsomes and involvement of cytochrome P-450 in dehydrogenation of lovastatin. *Drug Metab. Dispos.* **18,** 218–222 (1990).
20. H. Y. Pan, A. R. DeVault, D. Wang-Iverson, E. Ivashkiv, B. N. Swanson, and A. A. Sugerman: Comparative pharmacokinetics and pharmacodynamics of pravastatin and lovastatin. *J. Clin. Pharmacol.* **30,** 1128–1135 (1990).